Article

Cell Reports

Activation of CDK4 Triggers Development of Non-alcoholic Fatty Liver Disease

Graphical Abstract

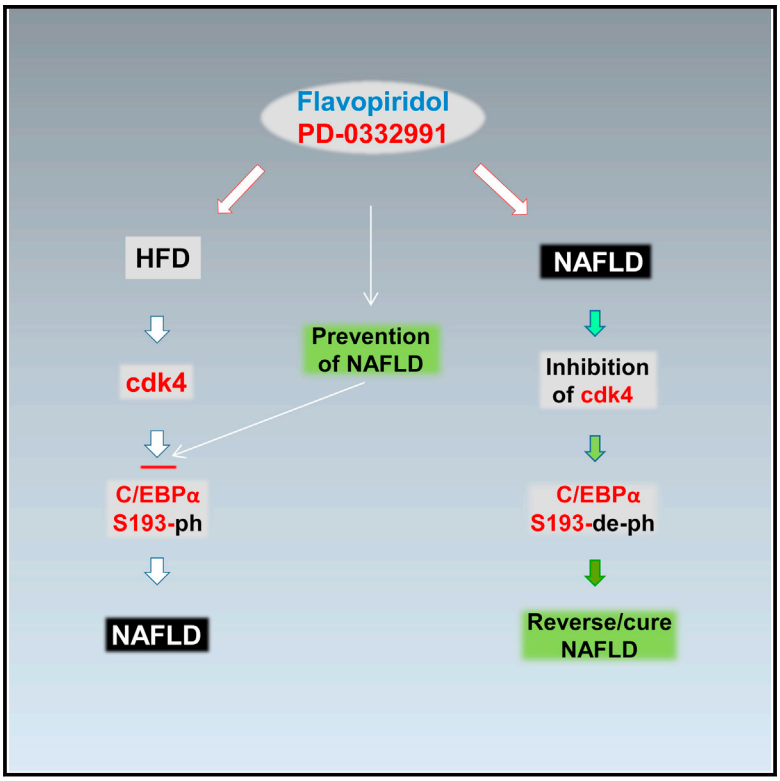

Authors

Jingling Jin, Leila Valanejad, Thuy Phuong Nguyen, ..., Lauren Stock, Lubov Timchenko, Nikolai A. Timchenko

Correspondence

nikolai.timchenko@cchmc.org

In Brief

Jin et al. show that cdk4 activation triggers non-alcoholic fatty liver disease (NAFLD) development. They find that an increased level of cdk4 protein in mice and humans leads to C/EBPα-p300 complex formation and hepatic steatosis. Disruption of this pathway or inhibition of cdk4 prevents NAFLD development and reverses steatosis.

Highlights

- HFD activates cdk2 and cdk4 and causes liver proliferation and NAFLD
- Increase in Cdk4 protein level is a key event in NAFLD development
- Inhibition of cdk2/cdk4 prevents development of hepatic steatosis
- Inhibition of cdk4 in livers with existing steatosis reverses the steatosis

Jin et al., 2016, Cell Reports *16*, 744–756
July 19, 2016
http://dx.doi.org/10.1016/j.celrep.2016.06.019

OPEN ACCESS
CellPress

Cell Reports
Article

Activation of CDK4 Triggers Development of Non-alcoholic Fatty Liver Disease

Jingling Jin,[3,4] Leila Valanejad,[1,4] Thuy Phuong Nguyen,[1,4] Kyle Lewis,[1,3] Mary Wright,[1] Ashley Cast,[1] Lauren Stock,[2] Lubov Timchenko,[2] and Nikolai A. Timchenko[1,3,*]
[1]Division of Pediatric General and Thoracic Surgery
[2]Department of Neurology
Cincinnati Children's Hospital Medical Center (CCHMC), 3333 Burnet Avenue ML 7015, Cincinnati, OH 45229, USA
[3]Huffington Center on Aging, Baylor College of Medicine, One Baylor Plaza, Houston, TX 77030, USA
[4]Co-first author
*Correspondence: nikolai.timchenko@cchmc.org
http://dx.doi.org/10.1016/j.celrep.2016.06.019

SUMMARY

The development of non-alcoholic fatty liver disease (NAFLD) is a multiple step process. Here, we show that activation of cdk4 triggers the development of NAFLD. We found that cdk4 protein levels are elevated in mouse models of NAFLD and in patients with fatty livers. This increase leads to C/EBPα phosphorylation on Ser193 and formation of C/EBPα-p300 complexes, resulting in hepatic steatosis, fibrosis, and hepatocellular carcinoma (HCC). The disruption of this pathway in cdk4-resistant C/EBPα-S193A mice dramatically reduces development of high-fat diet (HFD)-mediated NAFLD. In addition, inhibition of cdk4 by flavopiridol or PD-0332991 significantly reduces development of hepatic steatosis, the first step of NAFLD. Thus, this study reveals that activation of cdk4 triggers NAFLD and that inhibitors of cdk4 may be used for the prevention/treatment of NAFLD.

INTRODUCTION

NAFLD generally develops under conditions of high-fat diet (HFD) and aging as the disease progresses over several stages. The first stage is the development of hepatic steatosis, which is characterized by an accumulation of triglycerides (TGs) in the cytoplasm of hepatocytes. Hepatic steatosis can further progress to non-alcoholic steatohepatitis (NASH) and ultimately to cirrhosis and hepatocellular carcinoma (HCC) if not treated or prevented (Cohen et al., 2011; Hebbard and George, 2011). With advanced age, patients develop hepatic steatosis and have an increased risk in developing liver cancer (Schmucker, 2005; Timchenko, 2011). Accumulation of fat in the liver (hepatic steatosis) might be a result of multiple alterations of fat metabolism, including enhanced fat uptake, increased lipogenesis, and decreased secretion of very-low-density lipoproteins (Cohen et al., 2011).

C/EBPα and C/EBPβ are two members of the C/EBP family. Members of this protein family contain a basic region and a leucine zipper region (Johnson, 2005), and they dimerize and control multiple functions in different tissues. C/EBPα is required for liver differentiation, where it acts as a strong inhibitor of liver proliferation (Timchenko, 2009; Wang et al., 2006). The biological activities of C/EBPα are mainly controlled by post-translational modifications. Among several important modification sites is Ser193, a key amino acid of C/EBPα through which multiple functions of C/EBPα are regulated, including its role in the biology of the liver (Wang and Timchenko, 2005; Jin et al., 2010; Wang et al., 2010). It has been shown that cyclin D3-cyclin-dependent kinase 4 (cdk4) phosphorylates C/EBPα on Ser193, causing C/EBPα to associate with the chromatin remodeling protein p300. C/EBPα-p300 complex formation results in alterations of chromatin structure (Jin et al., 2010) that, in turn, lead to C/EBPα-dependent growth arrest (Wang et al., 2010, Jin et al., 2010). Our recent paper (Jin et al., 2013) showed that phosphorylation of C/EBPα at Ser193 regulates steatosis.

An important regulator of C/EBPα activity, cdk4 is activated by D-type cyclins (D1 and D3) and mediates progression of the cell cycle through G1 phase by phosphorylation of retinoblastoma protein (Rb) and subsequent release of Rb-dependent repression of S-phase genes (Baker and Reddy, 2012). Cdk4 and cdk6 are highly homologous and share many properties. Therefore, the majority of the information about cdk6 also applies to cdk4. Crystal structures of the p16-cdk6 complexes revealed that p16 interacts with amino acid residues located in the active sites of cdk4 and cdk6 and diminishes kinase activities of cdk4 and cdk6 (Gil and Peters, 2006; Endicott et al., 1999). A systematic screen for cdk4/cdk6 substrates in HEK293 cells identified a broad number of substrates (Anders et al., 2011). Since cdk4 is involved in the development of cancer, cdk4 inhibition is under intensive investigation for cancer therapy. The initial development of cdk4/6 inhibitors led to the discovery of the first generation of inhibitors, such as flavopiridol (FPD) and roscovitine (Dickson and Schwartz, 2009). Further research for more specific and non-toxic inhibitors has identified a small compound, PD-0332991, which seems to be the best inhibitor of cdk4/6. It has been shown that PD-0332991 causes G1 growth arrest by blocking phosphorylation of Rb (Rivadeneira et al., 2010).

In this study, we found that the triggering event in the development of HFD-mediated NAFLD is the elevation of cdk4 and subsequent promotion of C/EBPα-p300 complexes. Disruption of this pathway by genetic mutation of C/EBPα and by inhibition of cdk4 significantly inhibits the development of NAFLD.

RESULTS

Cdk4 Is Activated by HFD and Phosphorylates C/EBPα at Ser193, Leading to an Increase of C/EBPα-p300 Complexes

We have shown previously that the elevation of C/EBPα-p300 complexes is involved in the development of hepatic steatosis. Since cdk4 phosphorylates Ser193 and increases the formation of C/EBPα-p300 complexes (Jin et al., 2013), we examined if cdk4 is activated in wild-type (WT) mice during the development of NAFLD under HFD conditions. WT mice were treated with HFD for 3 and 12 weeks, and livers were harvested and examined for the expression of proteins of the cyclin D3-cdk4-C/EBP-p300 pathway. Representative results are shown in Figure 1A. We found that both cyclin D3 and cdk4 are elevated at 3 and 12 weeks of HFD and that this elevation leads to increased phosphorylation of C/EBPα at Ser193. Co-immunoprecipitation (coIP) studies showed that amounts of C/EBPα-p300 complexes are increased in livers of mice at 3 and 12 weeks of HFD (Figure 1B). Note that levels of C/EBPα, C/EBPβ, and p300 also were increased at 3 and 12 weeks of HFD. However, these proteins form a tripartite complex only if C/EBPα is phosphorylated at Ser193 (Jin et al., 2013, 2015). Based on these data, we hypothesized that cdk4 is a key protein that increases C/EBPα-p300 complexes under conditions of HFD in mice, leading to NAFLD.

Cdk4-C/EBPα-p300 Pathway Is Activated in Patients with NAFLD

Given activation of cdk4-C/EBPα-p300 in HFD-mediated NAFLD in mice, we next asked if this pathway is activated in livers of patients with NAFLD. Western blotting with nuclear extracts isolated from control livers and from livers of NAFLD patients showed that cdk4 is significantly increased in NAFLD patients (Figure 1C). Calculation of cdk4 as a ratio to β-actin revealed that cdk4 is 6- to 8-fold elevated in livers of patients with NAFLD. We next examined cdk4 expression in two control livers and in four livers from patients with NAFLD using immunostaining approaches. This assay showed that cdk4 is increased in all examined samples from patients with fatty liver disease (Figure 1D).

We have shown previously that human C/EBPα is phosphorylated at Ser190 in the livers of these patients (Jin et al., 2013). Therefore, we next examined if this phosphorylation might result in the formation of C/EBPα-p300 complexes using the coIP approach. We found that amounts of these complexes are increased in livers of NAFLD patients (Figure 1E). Because the C/EBPα-p300 complexes activate promoters of enzymes of TG synthesis, we examined expression of key enzymes GPAT and DGAT2, which catalyze the first and last steps of TG synthesis. Figure 1F shows that expression of both enzymes is increased in livers of patients with NAFLD. Thus, these data demonstrated that the cdk4-C/EBPα-p300 pathway is activated in patients with NAFLD and correlates with the elevation of enzymes of TG synthesis. From the results obtained in mice and data collected in humans, we hypothesized that cdk4 might be a key triggering event in the development of hepatic steatosis and further stages of NAFLD (Figure 1G).

HFD-Mediated Hepatic Steatosis Is Inhibited in Cdk4-Resistant S193A Mice

To examine if cdk4-dependent phosphorylation of C/EBPα at Ser193 is involved in the development of NAFLD, we utilized two knockin mouse models: constitutively active C/EBPα-S193D mice (Wang et al., 2010; Jin et al., 2010) and recently generated cdk4-resistant C/EBPα-S193A mice (Jin et al., 2015). Due to the fact that C/EBPα cannot be phosphorylated at Ser193 by cdk4 in S193A mice, we first examined if these mice expressing cdk4-independent C/EBPα might be resistant to the development of hepatic steatosis in a short time frame of HFD protocol. We treated S193A mice with HFD for 3 and 12 weeks. An identical treatment was performed with S193D mice and with WT mice as the controls.

Figure 2A shows H&E and oil red O staining of livers under normal diet (ND) and 3 and 12 weeks of HFD. In agreement with previous observations, WT mice developed steatosis at 3 and 12 weeks while S193D mice had much stronger steatosis at the same time points. In S193A mice, however, both H&E and oil red O staining showed no steatosis at 3 weeks and a much weaker steatosis at 12 weeks. These data indicate that knockin mice expressing the cdk4-resistant C/EBPα-S193A mutant are also resistant for development of hepatic steatosis within 12 weeks of HFD. Since steatosis is inhibited in S193A mice and because these mice have reduced basal levels of glucose (Jin et al., 2013), we asked if these animals might have changes in insulin sensitivity. Therefore, we performed an insulin tolerance test (ITT); however, no differences were detected in insulin sensitivity between WT and S193A mice. Insulin-mediated glucose lowering was identical in both groups (Figure 2B). Note that, while the ITT showed the reduction of the glucose as a percentage to the levels observed before insulin injection, the levels of glucose were lower in S193A mice during the entire duration of the test (Figure S1).

Cdk4-Resistant S193A Mice Do Not Accumulate C/EBPα-p300 Complexes

We next determined a molecular basis for the resistance of S193A mice to develop steatosis. We first examined if cdk4 and cyclin D3 are properly activated in S193A mice. Similar to WT mice, both these proteins were increased in livers of S193A mice at 3 and 12 weeks of HFD (Figures 2C and 2E). Examination of C/EBPα and p300 proteins also showed that they are elevated in WT and S193A mice at 3 and 12 weeks, with a slightly lower elevation in S193A mice. In agreement with observations shown in Figures 1A and 1B, coIP studies revealed that C/EBPα-p300 complexes are elevated in WT mice; however, these complexes were not detectable in livers of S193A mice after HFD treatments (Figure 2C). These data clearly demonstrated that the mutation of S193 to Ala blocked the formation of C/EBPα-p300 complexes in the animals under HFD protocol.

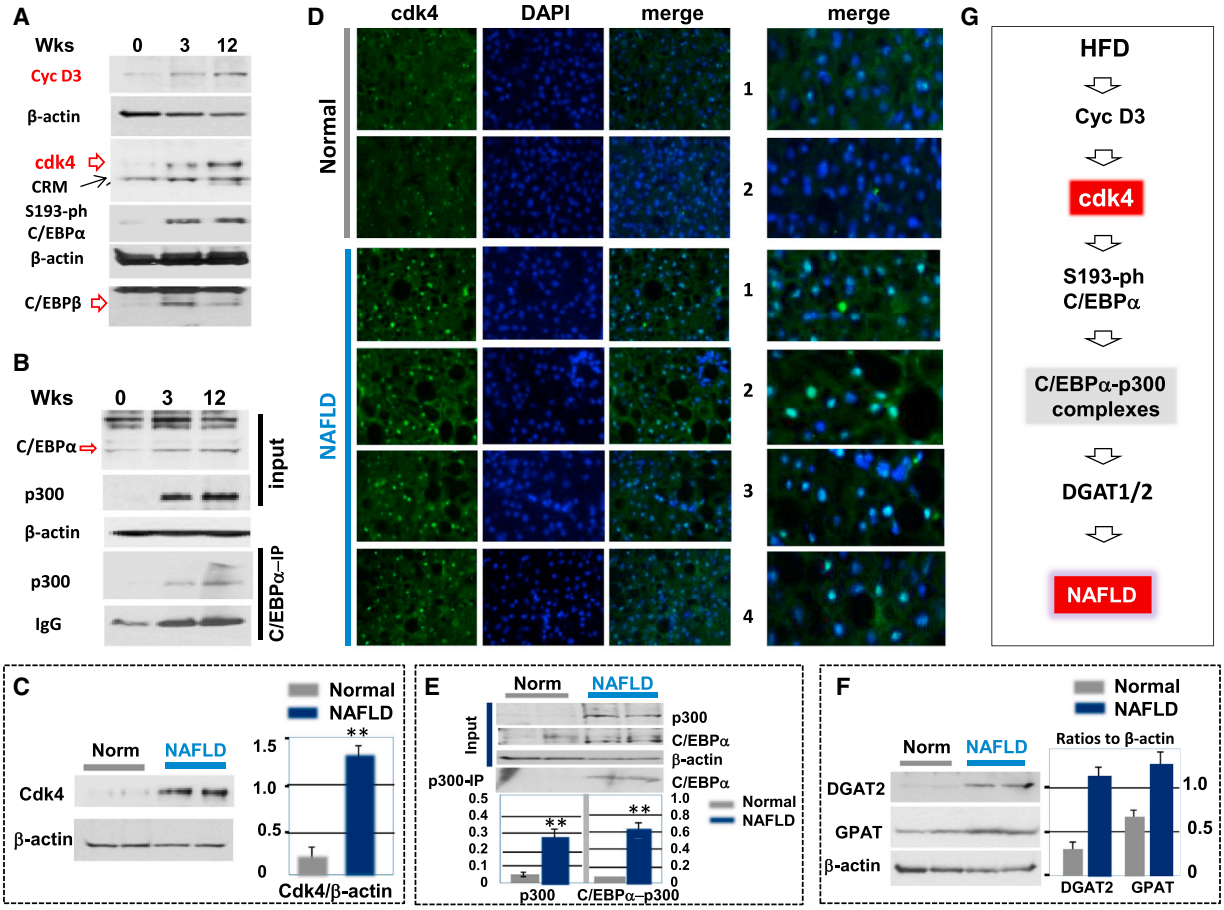

Figure 1. Cdk4 Is Activated in Animal Models of NAFLD and in Patients with NAFLD

(A) Cyclin D3/cdk4-C/EBP-p300 pathway is activated in mouse livers after HFD treatment. Western blotting shows that cyclinD3, cdk4, ph-C/EBPα, and p300 are increased in livers after HFD treatment.

(B) C/EBPα-p300 complexes are elevated during development of hepatic steatosis in mice. C/EBPα was immunoprecipitated from nuclear extracts and immunoprecipitates were examined by western blotting with antibodies to p300. Upper image shows input of the proteins (IgG, signals of immunoglobulins on the immunoprecipitate membranes). Images in (A) and (B) represent typical pictures of three independent experiments with three mice at each time point. Examination of additional mice is shown in Figure 2C.

(C) Protein levels of cdk4 are increased in livers of patients with fatty liver disease. Western blotting was performed with total protein extracts isolated from the livers. The membrane was re-probed with antibodies to β-actin. Bar graph shows a summary of three independent experiments.

(D) Immunostaining of normal livers and livers from four patients with fatty liver diseases using antibodies to cdk4. The slides were stained with DAPI. The right panel shows enlarged pictures of merged images.

(E) Protein levels of p300 and C/EBPα-p300 complexes are increased in livers of patients with fatty liver diseases. Upper image: western blotting was performed with total protein extracts isolated from the livers. The membrane was re-probed with antibodies to β-actin. Bar graphs show calculations of p300 and C/EBPα-p300 complexes as ratios to β-actin.

(F) Amounts of DGAT2 and GPAT are increased in livers of patients with fatty liver diseases. Western blotting was performed with total protein extracts isolated from the livers. The membranes were re-probed with antibodies to β-actin. Bar graph shows levels of GPAT and DGAT2 as ratios to β-actin.

(G) A model shows hypothetical mechanisms for the development of NAFLD (see Results).

The Lack of C/EBPα-p300 Complexes Resulted in the Failure of S193A Mice to Activate Enzymes of TG Synthesis and Enzymes of Glucose Synthesis

Our previous studies have shown that C/EBPα-p300 complex is a positive regulator of enzymes of TG synthesis, GPAT and DGAT1/2 (Jin et al., 2013), and enzymes of glucose synthesis, PEPCK and G6-phase (Jin et al., 2015). The reduction of G6-phase in S193A mice also recently has been reported (Fleet et al., 2015). Since these proteins are key regulators of hepatic steatosis, we asked if their levels might be changed in livers of S193A mice under conditions of HFD protocol. We found that GPAT, DGAT1, DGAT2, PEPCK, and G6-phase are elevated in livers of WT mice at 3 and 12 weeks of HFD; however, no elevation of these proteins was detected in livers of S193A mice (Figure 2D). Since GPAT, DGAT1, and DGAT2 are key enzymes of TG synthesis, the failure of activation of these proteins by p300-C/EBPα complexes in S193A mice seems to be the main mechanism of the inhibition of hepatic steatosis.

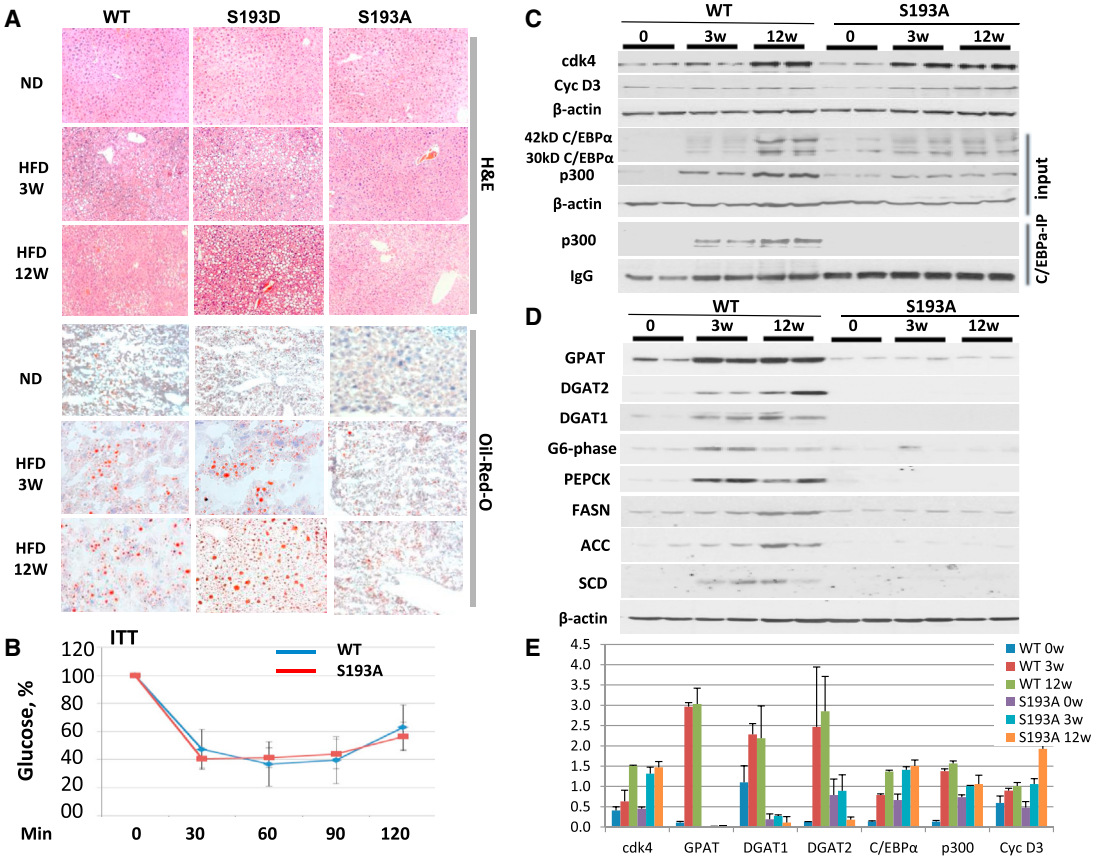

Figure 2. Cdk4-Resistant C/EBPα-S193A Mice Do Not Develop Hepatic Steatosis under Conditions of an HFD Protocol

(A) S193A mice do not develop hepatic steatosis, while S193D mice are developing hepatic steatosis much faster than WT mice after 3 and 12 weeks of HFD conditions. Typical pictures of H&E and oil red O staining of WT, S193D, and S193A livers (five mice of each genotype) are shown at 3 and 12 weeks after the initiation of an HFD. Scale bar, 40 μm.

(B) Insulin-dependent lowering of glucose is not affected in S193A mice. ITT was performed with WT and S193A mice as shown in the Supplemental Experimental Procedures.

(C) Cyclin D3-cdk4 pathway is identically elevated in WT and S193A mice, but C/EBPα-p300 complexes are not formed in livers of S193A mice. Western blotting was performed with antibodies to cdk4, cyclin D3, C/EBPα, and p300. Bottom image: C/EBPα was immunoprecipitated from nuclear extracts and p300 was examined in these immunoprecipitates. IgG, signals of immunoglobulins detected on the membrane.

(D) Expression of enzymes of TG synthesis, glucose synthesis, and lipid metabolism. Cytoplasmic extracts from WT and S193A mice were probed with antibodies shown on the left. Membranes were re-probed with antibodies to β-actin.

(E) Levels of proteins in (C) and (D) were calculated as ratios to β-actin. The bar graph shows a summary of three repeats with three mice per time point. Additional calculations are shown in Figure S2.

To further investigate if other lipogenic pathways are altered in S193A mice, we examined the expression of FASN, ACC, and SCD by western blotting, and we found that these lipogenic pathways are activated in livers of WT mice at 3 and 12 weeks but livers of S193A mice do not increase expression of these proteins (Figure 2D). Thus, these data revealed that cdk4-resistant S193A mice do not develop hepatic steatosis under HFD protocol and that this correlates with a failure to form the C/EBPα-p300 complexes and to activate genes that are involved in the development of hepatic steatosis.

Development of HFD-Mediated Fibrosis Is Inhibited in S193A Mice

It has been shown that long-term treatments of mice with HFD leads to further development of NAFLD, including progression to fibrosis, cirrhosis, and HCC. Therefore, we next examined if disruption of the cdk4-C/EBPα pathway in S193A mice might affect the development of fibrosis under an HFD protocol. Previous studies showed that fibrosis is very well developed in mouse livers at 6–7 months after the initiation of an HFD protocol (Hill-Baskin et al., 2009). Therefore, we fed WT, S193D, and S193A mice with an HFD for 7 months and examined fibrosis using several approaches. H&E and oil red O staining showed that, while WT and S193D mice have significant accumulation of fat droplets, the development of hepatic steatosis is weaker in S193A mice (Figure 3A). Examination of livers under a higher magnification showed that there are detectable differences in the liver structure (Figure 3B). We next examined development of fibrosis by staining livers with Sirius Red, and we found that the development of fibrosis is significantly inhibited in S193A mice (Figure 3A).

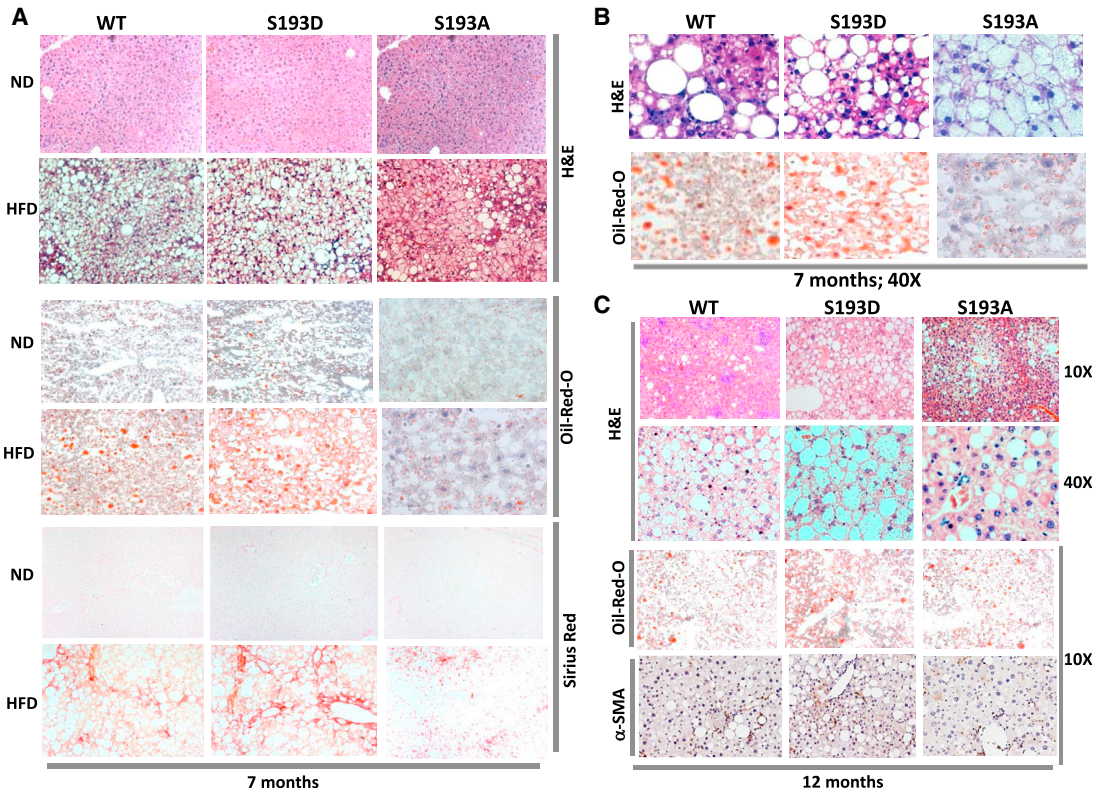

Figure 3. Development of NAFLD and Fibrosis Is Inhibited in S193A Mice after 7 and 12 Months of HFD Treatments

(A) Typical pictures of H&E, oil red O, and Sirius Red staining of WT, S193D, and S193A livers under HFD conditions. Upper image shows H&E staining of the livers, middle image shows oil red O staining, and bottom image shows Sirius Red staining. Scale bar, 40 μm.

(B) Sections of H&E staining under high magnification are shown.

(C) Typical pictures of H&E and oil red O staining of WT, S193D, and S193A livers under 12 months of HFD conditions. Upper image shows H&E staining of the livers and bottom image shows oil red O and α-SMA staining. The figure shows typical pictures obtained with livers of five mice of each genotype. Scale bar, 40 μm.

C/EBPα-S193A Mice Have Reduced Hepatic Steatosis at 12 Months of HFD

We next studied the development of NAFLD in S193A mice after very long treatments with HFD. For this goal, five mice of each genotype were treated with HFD for 48 weeks (12 months). All animals survived these long treatments, but WT and S193D mice were fatty and, as expected, developed liver disease. H&E staining showed that S193D mice developed severe macrovesicular steatosis and that liver architecture was significantly destroyed with significant loss of hepatocytes (Figure 3C). Livers of WT mice also developed these disorders but to a lesser degree. Contrary to these two mouse lines, S193A livers had much less steatosis and relatively abundant hepatocytes (Figure 3C). Oil red O staining confirmed that development of steatosis is inhibited in S193A livers after 12 months of HFD protocol. Examination by α-SMA staining showed that the development of fibrosis is also inhibited in S193A mice (Figure 3C).

NAFLD Is Reduced but Liver Proliferation Is Increased in S193A Mice after 12 Months of HFD

The 12-month duration of HFD protocol usually initiates development of liver cancer. One of the characteristics of liver cancer is increased liver proliferation. To examine the degree of liver proliferation in our animal models, we performed a set of studies using several approaches. First, we calculated number of mitotic figures and found that all three mouse models have increased mitosis after 12 months of HFD, but the levels of mitosis are different. Despite higher steatosis, the mitosis in S193D mice was lower than in WT mice. On the contrary, cdk4-resistant S193A mice had higher levels of proliferation but much less steatosis (Figures 4A and 4B). Second, we performed ki67 staining and found that proliferation of S193A hepatocytes is significantly higher than one of WT livers, while S193D mice have a reduced number of ki67-positive hepatocytes (Figures 4A and 4B). These results are consistent with growth-inhibitory/tumor-suppressive activities of C/EBPα mutants S193D and S193A (Wang et al., 2010; Jin et al., 2015), and they suggest that the S193D mutant inhibits liver proliferation under HFD protocol while S193A does not.

We next examined expression of cdk4 and phosphorylation status of C/EBPα in our animal models after 7 and 12 months of HFD treatments. In these studies, we incorporated protein extracts of 3-month-HFD-treated mice. Figure 4D shows that cdk4 was activated in all three mouse lines and that C/EBPα

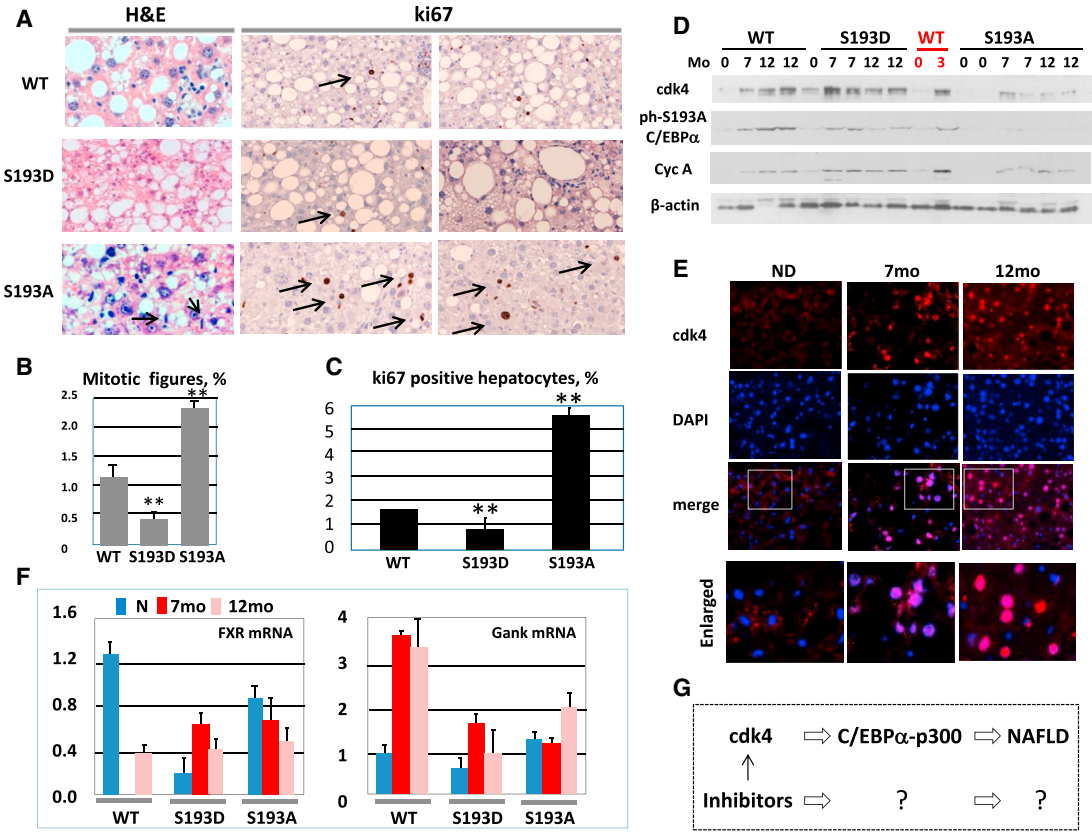

Figure 4. 12-Month Treatments with an HFD Lead to Increased Liver Proliferation and Initiation of Cancer-Specific FXR-Gank Pathway

(A) Left panel: H&E staining shows mitotic figures. Middle and right panels: ki67 staining of livers after 12 months of HFD is shown.

(B) Bar graph shows numbers of mitotic figures in WT, S193D, and S193A mice per 1,000 hepatocytes.

(C) Bar graph shows percentages of ki67-positive hepatocytes. Three animals of each genotype were used for calculations of mitotic figures and BrdU uptake.

(D) The cdk4-cyclin D3 pathway in WT, S193D, and S193A mice at 7 and 12 months after the initiation of an HFD protocol. Nuclear extracts were isolated from livers and used for western blotting with Abs shown on the left.

(E) Amounts of cdk4 are increased in nuclei of hepatocytes after HFD treatment. Liver sections were stained with antibodies to cdk4 and with DAPI. Enlarged images of merged pictures are shown on the bottom.

(F) Cancer-specific FXR-Gank pathway is activated in WT, S193D, and S193A mice after 7 and 12 months of an HFD. Expression of FXR and Gankyrin was determined in livers after 7 and 12 months of an HFD. Three animals for each genotype were used in these experiments.

(G) A diagram summarizes the examination of mechanisms of NAFLD in genetically modified animal models.

was phosphorylated at Ser193 in WT mice, but not in S193A mice. Interestingly, ph-S193-specific antibodies also recognized the S193D mutant, which was reduced at 12 months of HFD in livers of S193D mice. Examination of cyclin A as an indicator of proliferation revealed that cyclin A is increased in all mouse lines at 7 and 12 months of HFD. In these studies, we found that cyclin A also is activated in WT mice after 3 months of HFD protocol. To examine intracellular localization of cdk4 after 12 months of HFD, we immunostained livers of WT mice with antibodies to cdk4. This assay confirmed that cdk4 is significantly increased in livers of HFD-treated mice at 7 and 12 months and that the major fraction of cdk4 is located in the nucleus (Figure 4E).

Our previous observations were that the development of liver cancer under conditions of DEN-mediated carcinogenesis is facilitated by a downregulation of farnesoid X receptor FXR and upregulation of an oncogene Gankyrin, Gank (Jiang et al., 2013). To examine if this pathway of liver cancer is initiated after 7 and 12 months of HFD, we used qRT-PCR approach with mRNA isolated from WT, S193D, and S193A mice. In WT mice, we detected a dramatic reduction of FXR at 7 months and a 3-fold reduction at 12 months. In agreement with the role of FXR as a repressor of Gank, the levels of Gank were 2- to 4-fold elevated in WT mice at 7 and 12 months of HFD. Examination of S193D and S193A mice surprisingly showed that FXR is reduced in both these lines without treatments; but, it was slightly elevated in S193D and reduced in S193A mice compared to non-treated animals (Figure 4F). However, comparisons to the levels of FXR in WT non-treated mice showed that levels of FXR are reduced in all three mouse lines after 7 and 12 months of an HFD protocol. We also found that levels of Gank are elevated in both S193D and S193A mice at 12 months after the initiation of an HFD protocol (Figure 4F). Taken together, these data demonstrated that 12-month HFD treatments of all three mouse lines lead to the severe steatosis in WT and S193D mice and that

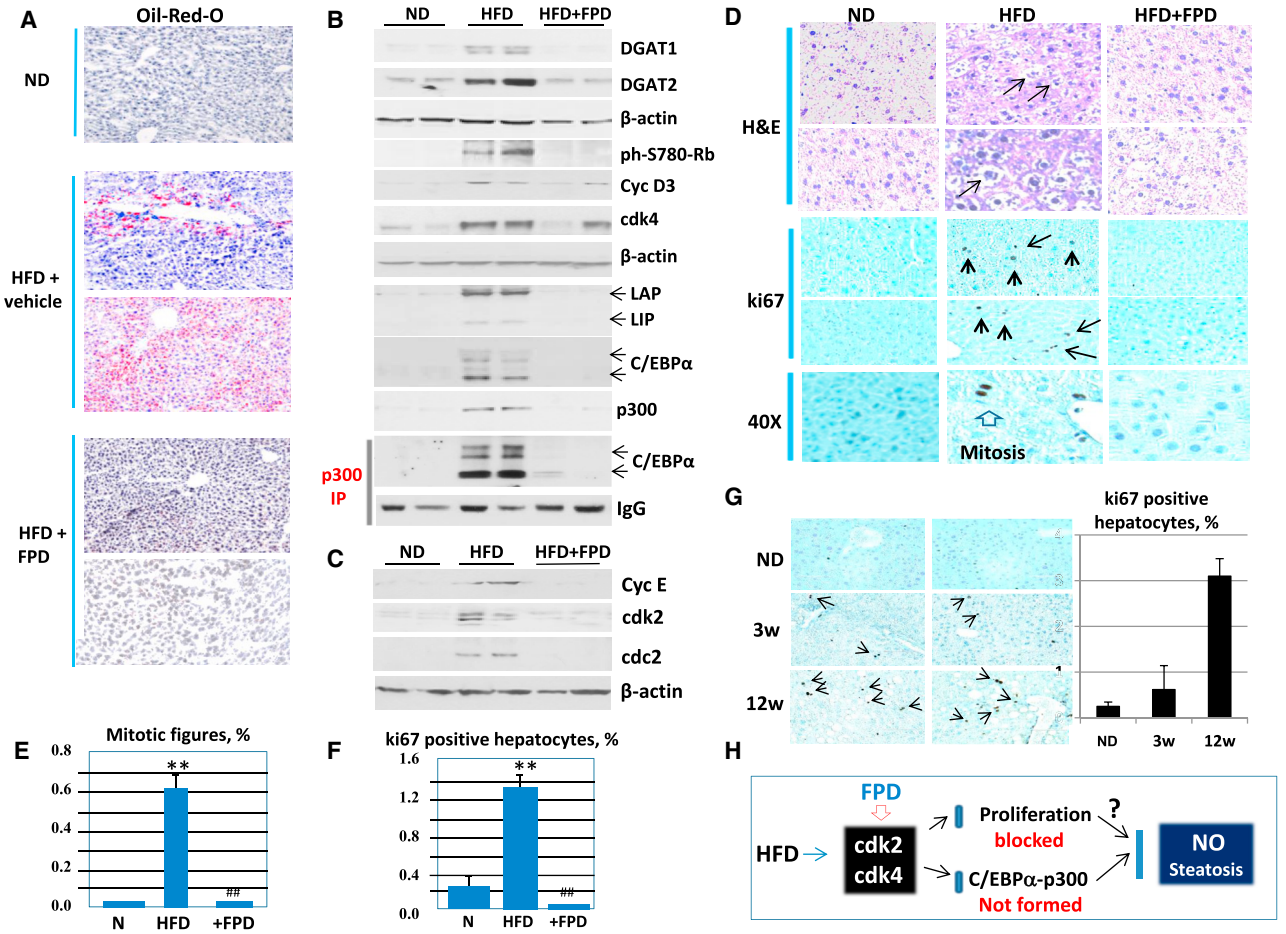

Figure 5. Inhibition of Cdk2/Cdk4 Activities by FPD Prevents Development of Hepatic Steatosis and Inhibits Liver Proliferation

(A) Oil red O staining of livers of mice treated with normal diet (ND), with HFD + vehicle, and with HFD + FPD is shown.

(B) Western blotting of protein extracts with antibodies to enzymes of TG synthesis, DGAT1 and DGAT2, and examination of cdk4-C/EBPα pathway in livers of mice treated with HFD and HFD + FPD. Western blotting was performed with Ab shown on the right. LAP and LIP are isoforms of C/EBPβ. Bottom image shows coIP studies in which p300 was immunoprecipitated and C/EBPα was examined in these immunoprecipitates.

(C) Expression of cell-cycle proteins was examined by western blotting.

(D) H&E and ki67 staining of livers of mice treated with ND, with HFD, and with HFD + FPD. 40× shows ki67 staining under 40× magnification.

(E) Percentages of mitotic figures are shown.

(F) Percentages of ki67-positive hepatocytes. Four animals of each group were used for calculations of mitotic figures and ki67 staining.

(G) Liver proliferation was examined in mice after 3 and 12 weeks of an HFD using ki67 staining. Left images show typical pictures of ki67 staining. Bar graph shows percentages of ki67-positive hepatocytes.

(H) A diagram summarizes examination of effects of FPD on HFD-mediated steatosis and liver proliferation.

steatosis is inhibited in livers of S193A mice. We also found that liver proliferation is significantly increased and cancer-specific FXR-Gank pathway is activated in all three lines; however, liver proliferation was not strongly activated in S193D mice due to growth-inhibitory activity of this mutant.

Inhibition of Cdk4 by FPD Prevents Development of the First Stage of NAFLD, Hepatic Steatosis

Figure 4G summarizes the examination of HFD-mediated NAFLD in our animal models. Given a strong inhibition of NAFLD in cdk4-resistant C/EBPα-S193A mice, we asked if the inhibition of cdk4 by pharmacological intervention might reduce the development of hepatic steatosis (Figure 4G) in the mice under HFD protocol. In the first set of experiments, we used FPD as the inhibitor of cdk4. Note that FPD also inhibits cdk2 (Nagaria et al., 2013; Luke et al., 2012). Control WT mice were treated with HFD, while experimental mice were treated with HFD plus FPD for 5 weeks. Examination of livers by oil red O staining showed that control mice develop hepatic steatosis; however, FPD-treated mice did not show detectable steatosis (Figure 5A). Examination of enzymes of TG syntheses DGAT1 and DGAT2 showed significant increases in HFD control mice, but no elevation was observed in livers of mice treated with FPD (Figure 5B). To examine if FPD inhibits the activity of cdk4, we performed western blotting with antibodies to a target of cdk4, ph-780-Rb protein. These data revealed that HFD-mediated activation of

cdk4 leads to significant phosphorylation of Rb, FPD completely inhibits cdk4 activity, and phosphorylated forms of Rb are not detectable in livers of mice treated with FPD (Figure 5B).

We next examined cdk4-C/EBPα-p300 pathway in livers of control and FPD-treated mice. Although our original hypothesis was that the inhibition of cdk4 by FPD might block phosphorylation of C/EBPα and subsequent formation of complexes with p300, we were surprised to find that the inhibition of cdk2/cdk4 by FPD has a much broader and much stronger effect on the expression of several components that are involved in the formation of C/EBPα-p300 complexes. Particularly, we observed that FPD inhibits HFD-mediated elevation of cyclin D3, C/EBPα, C/EBPβ, and p300, while these proteins are elevated in control HFD-treated mice (Figure 5B). In agreement with the reduction of C/EBPα and p300 proteins, we could not detect C/EBPα-p300 complexes in FPD-treated mice (Figure 5B). Given the unexpected results showing the reduction of protein levels of C/EBP proteins, which inhibit liver proliferation, we performed a careful examination of liver proliferation in WT mice. Examination of cell-cycle proteins showed activation of cyclin E, cdc2, and cdk2 in control mice treated by HFD; however, FPD completely blocked the activation of all these proteins (Figure 5C).

We also studied the number of mitotic figures and number of ki67-positive hepatocytes. In agreement with the effects of FPD on cell-cycle proteins, we observed that HFD significantly increases mitosis and number of ki67-positive hepatocytes and that FPD blocks this activation (Figures 5D–5F). Given these unexpected results showing the activation of liver proliferation by a very short treatment (5 weeks) with an HFD, we examined if proliferation of the liver was initiated in WT mice at early time points using animals shown in Figure 2. These animals were treated with an HFD for 3 and 12 weeks. Ki67 staining revealed that 3 weeks of HFD treatments are sufficient to initiate liver proliferation (Figure 5G). Figure 5H summarizes our examination of the effects of FPD on HFD-mediated steatosis. We found that HFD induces both liver proliferation, by activating cdk2/cdk4, and NAFLD, through elevation of p300-C/EBPα complexes. The inhibition of cdk2/cdk4 by FPD blocks the development of hepatic steatosis and liver proliferation.

Inhibition of Cdk4 by a More Specific Inhibitor, PD-0332991, Inhibits Development of HFD-Dependent Hepatic Steatosis, but Does Not Block Liver Proliferation

Our data for increase of liver proliferation are in agreement with a previous report showing that an HFD initiates liver proliferation, which correlates with inflammatory changes (Vansaun et al., 2013). Our data demonstrated that this elevation of proliferation occurs at very early time points (3 weeks after the initiation of an HFD protocol, Figure 5G), suggesting that this increase contributes to the further development of steatosis. To address this issue, we utilized a more specific inhibitor of cdk4, PD-0332991 (Flaherty et al., 2012; Leonard et al., 2012), in a similar setting of HFD-mediated steatosis. Note that we used a dose of PD-0332991 that was much lower than that described in the literature. Oil red O staining and western blotting with antibodies to DGAT1 and DGAT2 revealed that PD-0332991 (given with chow, 150 mg/kg chow) prevents the development of HFD-mediated hepatic steatosis (Figures 6A and 6B). To examine if this block of hepatic steatosis is mediated by the inhibition of cdk4 activity, we looked at the phosphorylation status of its targets Rb-Ser780 and C/EBPα-S193-ph. Western blotting with specific antibodies showed that both substrates are phosphorylated after treatments with HFD and that inhibition of cdk4 blocks or significantly reduces this phosphorylation (Figure 6B). CoIP studies revealed that the inhibition of cdk4 and reduction of S193-ph isoform of C/EBPα dramatically reduces C/EBPα-p300 complexes (Figure 6C).

We next examined if the inhibition of cdk4 by PD-0332991 blocks liver proliferation using three approaches. Examination of cell-cycle proteins, cyclin D1, cyclin D3, cdk2, and cdc2, and counting the number of ki67-positive hepatocytes showed that treatment with PD-0332991 does not prevent the increase of liver proliferation initiated by HFD (Figures 6B, 6D, and 6F). To get additional support for this result, we examined DNA replication by measuring BrdU uptake, and we found that PD-0332991 treatment does not inhibit liver proliferation under the conditions of our experiments (Figures 6E and 6G). Figure 6H shows a summary of these studies. We found that HFD-mediated hepatic steatosis and HFD/cdk2-4-mediated increase of liver proliferation are parallel events and that HFD-mediated liver proliferation does not seem to contribute to the development of hepatic steatosis. These data and the lack of C/EBPα-p300 complexes strongly suggest that the cdk4-C/EBPα-p300 signaling is the main cause of hepatic steatosis.

Inhibition of Cdk4 by PD-0332991 in Mice with Existing Hepatic Steatosis Reverses NAFLD

Although our data clearly show that inhibition of cdk4 prevents the development of hepatic steatosis, the next important question is if the inhibition of cdk4 might reverse existing steatosis. This is quite important because the patients with NAFLD need an approach to cure NAFLD. To test if the treatment with PD-0332991 reverses hepatic steatosis, we applied a strategy shown in Figure 7A. Four groups of mice were used for the 5- and 10-week duration of the treatments. The first group was fed an HFD for 5 weeks. The second group was fed an ND, while the third group was fed an HFD for the entire 10-week duration of the protocol. The fourth experimental group was fed an HFD for the first 5 weeks, and then an HFD plus PD-0332991 were given for the next 5 weeks. Animals were sacrificed 5 or 10 weeks after initiation of the protocol, and hepatic steatosis was examined by oil red O staining. Figure 7B shows that the 5-week-HFD group developed significant steatosis and that the 10-week-HFD group of mice further developed severe steatosis. However, inhibition of cdk4 by PD-0332991 dramatically reduced steatosis in the fourth group compared to both 5- and 10-week-HFD groups. Thus, these data demonstrated that inhibition of cdk4 reverses hepatic steatosis, even with continued treatments with an HFD.

We next examined the cdk4-C/EBPα pathway in mice treated for 10 weeks with an HFD and an HFD plus PD-0332991. Western blotting showed that, although protein levels of cdk4 are not reduced by PD-0332991, the activity of cdk4 is dramatically inhibited and Rb is not phosphorylated in mice treated with the inhibitor (Figure 7C). Consistent with oil red O results, amounts of

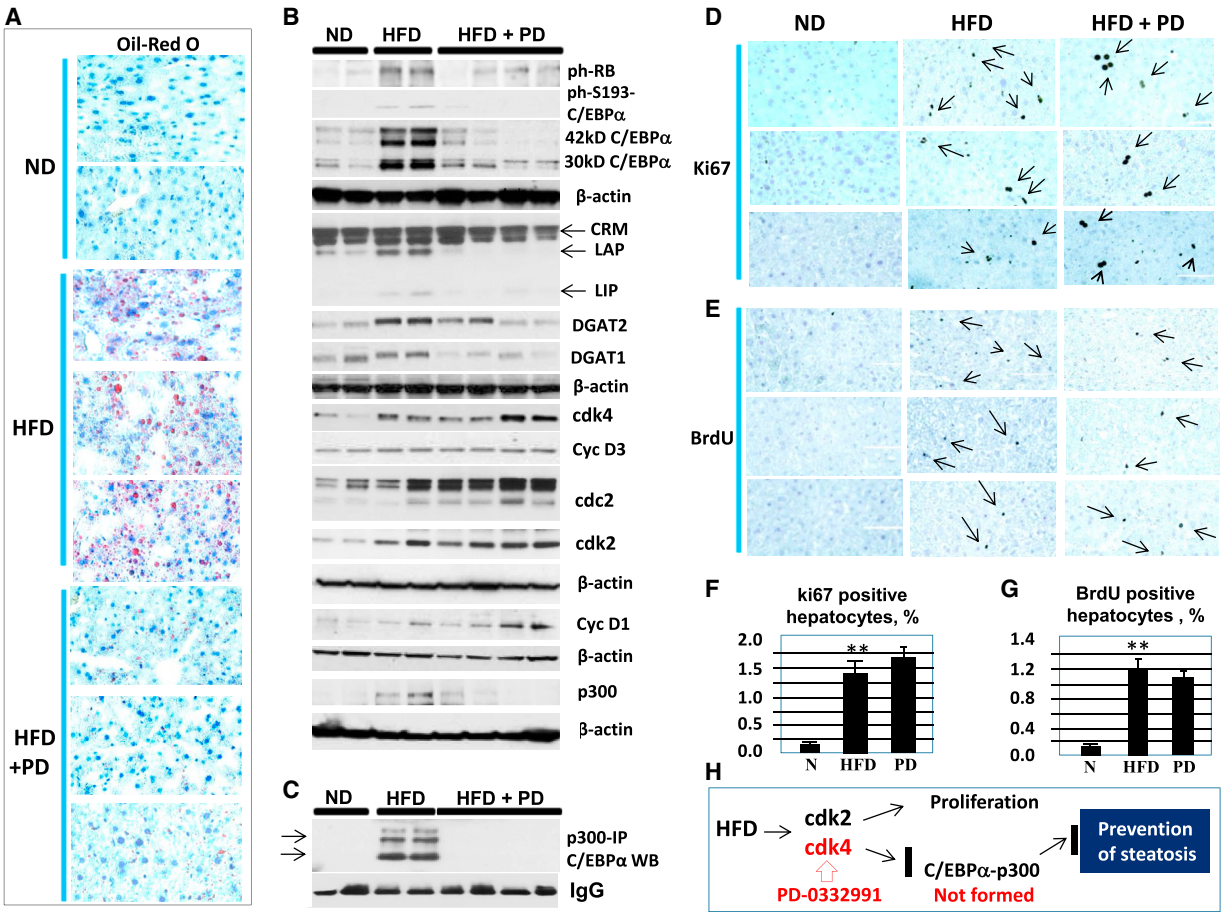

Figure 6. Inhibition of Cdk4 by Specific Inhibitor PD-0332991 Prevents Development of Steatosis, but Does Not Block Liver Proliferation

(A) Oil red O staining of mice treated with an ND, an HFD, and an HFD + PD-0332991 is shown.

(B) Western blotting with antibodies shown on the right. LAP and LIP are isoforms of C/EBPβ protein. CRM, cross-reactive molecule.

(C) Examination of C/EBPα-p300 complexes by coIP approach is shown.

(D and E) Examination of liver proliferation by (D) ki67 staining and (E) BrdU uptake. Typical pictures are shown.

(F and G) Bar graphs show percentages of (F) ki67-positive and (G) BrdU-positive hepatocytes.

(H) A diagram summarizing examination of effects of PD-0332991 on HFD-mediated steatosis and liver proliferation. Data in this figure show analyses of four to five mice of each group.

DGAT1 and DGAT2 proteins were reduced in mice treated with the inhibitor. We next examined C/EBPα-p300 complexes using the coIP approach. Figure 7D shows that C/EBPα-p300 complexes were significantly reduced or were not detectable in mice with inhibited cdk4 activity. These results clearly demonstrate that the PD-0332991-mediated reversal of hepatic steatosis is associated with the inhibition of cdk4 and with the subsequent reduction of C/EBPα-p300 complexes. Because an HFD also initiates liver proliferation, we asked if reversion of the steatosis by PD-0332991 involves the inhibition of liver proliferation. Three approaches were used: examination of cell-cycle proteins cdc2 and cdk2, BrdU uptake, and staining with antibodies to ki67. Figure 7C shows that levels of cdk2 and cdc2 were increased by HFD and that the inhibition of cdk4 in mice with existing steatosis did not reduce levels of these proteins. Figure 7E shows typical pictures of BrdU and ki67 staining. Calculations of BrdU-positive and ki67-positive hepatocytes showed that, at the low doses used in our experiments, PD-0332991 does not inhibit liver proliferation in the reversal experiments (Figures 7F and 7G). Taken together, these data revealed that PD-0332991-mediated inhibition of cdk4 reverses hepatic steatosis through the disruption of C/EBPα-p300 complexes, but does not affect the HFD-mediated proliferation of the liver (Figure 7H).

DISCUSSION

Recent methodological progress has determined a number of global changes that are associated with NAFLD (Hebbard and George, 2011). Despite this progress, very little is known about key events causing the development of NAFLD. NAFLD in humans is usually associated with age and inappropriate diet, which first lead to the development of hepatic steatosis and further progress into fibrosis, NASH, and HCC. One of the best

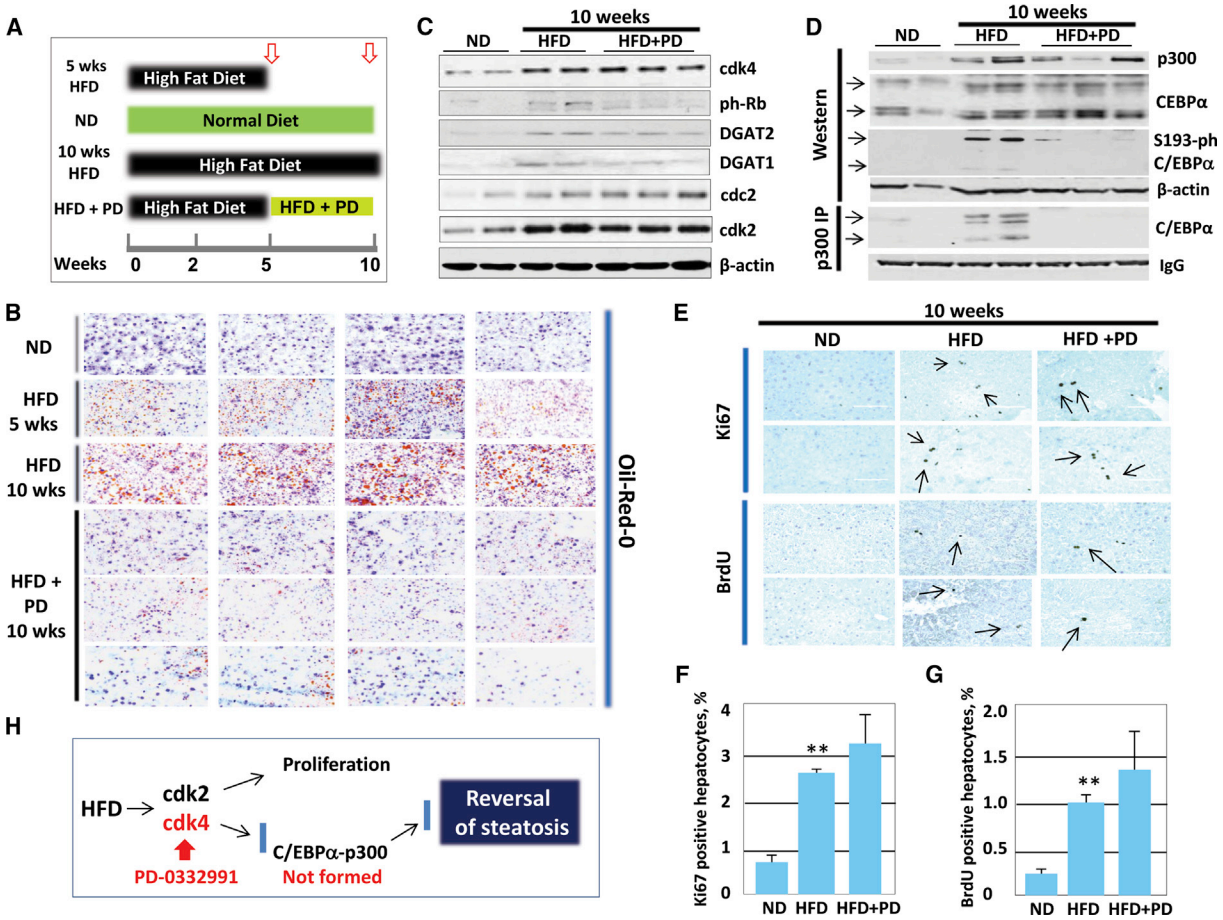

Figure 7. Inhibition of Cdk4 in Mice with Existing Hepatic Steatosis Dramatically Reduces Steatosis

(A) A diagram shows the strategy of experiments.

(B) Oil red O staining of livers. Typical pictures of four mice per group are shown.

(C) Inhibition of cdk4 activity by PD-0332991 and expression of DGAT1 and DGAT2 proteins. Western blotting was performed with Abs shown on the right.

(D) Inhibition of cdk4 activity by PD-0332991 reduces amounts of C/EBPα-p300 complexes. Input: western blotting with Abs to C/EBPα and p300 shows expression and input of these proteins. P300-IP: examination of p300 immunoprecipitates by western blotting with Abs to C/EBPα is shown. 42- and 30-kD C/EBPα isoforms are shown by arrows.

(E) Typical pictures show ki67 staining and BrdU uptake.

(F and G) Percentages of (F) ki67-positive and (G) BrdU-positive hepatocytes were calculated. Bar graphs represent summary of analyses of five mice per group.

(H) A diagram shows the results of reversion of HFD-mediated steatosis by PD-0332991-mediated inhibition of cdk4.

and biologically relevant animal models of NAFLD is the HFD treatment of mice. This treatment mimics the main steps of development of NAFLD in humans: hepatic steatosis, fibrosis, NASH, cirrhosis, and HCC. Transcription factors of the C/EBP family, C/EBPα and C/EBPβ, are key factors that are involved in the development of NAFLD.

We previously have generated two C/EBPα knockin mouse models in which Ser193 is mutated to Aspartate (S193D) and to Alanine (S193A). We found that S193D mice develop hepatic steatosis much faster than WT mice due to an elevation of C/EBPα/β-p300 complexes, which activate five enzymes of TG synthesis (Jin et al., 2013). This work suggested that there might be a kinase that is activated during the development of NAFLD and triggers NAFLD. In this paper, we have identified cdk4 as such kinase, which is activated in mouse models of NAFLD and in patients with fatty liver disease. Our paper presents experimental evidence showing that the inhibition of cdk4 by specific inhibitors and/or blocking of the phosphorylation of its downstream target C/EBPα by genetic mutation of Ser193 to Ala dramatically inhibits the development of NAFLD in animal models. These data clearly demonstrate that the inhibitors of cdk4 can be considered for the treatment of NAFLD in patients. It is interesting that cdk4 inhibitor PD-0332991 is used in clinical trials for the treatment of patients with liver cancer (Flaherty et al., 2012; Leonard et al., 2012), suggesting that it might be easily used for the treatment of NAFLD patients.

Although the HFD-mediated initiation of liver proliferation has been reported previously (Vansaun et al., 2013), the contribution of the liver proliferation to NAFLD had not been examined. We found that a very short treatment of mice with an HFD (3 weeks)

is sufficient to initiate liver proliferation. This finding raised the question if liver proliferation might contribute to the development of steatosis and further steps of NAFLD. Figures 5H, 6H, and 7H summarize our findings and present our hypotheses based on experiments with two inhibitors of cdk2/cdk4 and with genetically modified S193D and S193A mice. We found that increased liver proliferation is not involved in the development of hepatic steatosis. In fact, hepatic steatosis was much stronger in S193D mice, in which the proliferation was significantly lower than in WT and S193A mice (Figures 4A–4C). This opposite correlation suggests that the increased proliferation in WT mice might be a mechanism by which liver tries to block the development of NAFLD. It is also important to emphasize that our research identified a relationship between C/EBPα and FXR. Our results show that FXR is a downstream target of C/EBPα and that FXR is reduced in livers of animal models, S193A and S193D mice (Figure 4). Since many reports revealed that FXR is involved in the development of NAFLD (Carr and Reid, 2015; Xu et al., 2014), this finding suggests that the cdk4-C/EBPα pathway also might promote NAFLD through regulation of FXR.

The critical finding of our work is the identification of a key event in the development of NAFLD, which is the elevation/activation of cdk4. This finding and further work with inhibitors of cdk4 provide strong support for the consideration of cdk4 inhibition as a promising possible treatment, which prevents liver from the development of steatosis and might reduce existing steatosis. It is important to note that liver injury is one of the main causes of NAFLD. Our studies of cdk4-resistant C/EBPα-S193A mice showed significant inhibition of liver injury and the inhibition of steatosis at 7 and 12 months of an HFD protocol. On the contrary, knockin mice expressing constitutively active C/EBPα-S193D mutant have much more severe liver injury than WT or S193A mice, and they develop severe steatosis especially at 12 months after the initiation of an HFD. In experiments with prevention and the reversal of steatosis, we examined if inhibitors of cdk2/cdk4 might prevent/reverse liver injury. However, within the duration of these experiments (10 weeks), we did not detect alterations of ALT/AST in WT mice. We also performed TUNEL staining and immunoblotting of livers for activated caspase 3. Under the conditions of our experiments, these approaches did not detect liver injury within the 10-week duration of the HFD protocol. On the other hand, our experiments with Sirius Red detected a very minor staining of livers of WT mice treated with an HFD for 10 weeks, while this staining was not detected in animals treated with HFD plus PD-0332991 (Figure S3). Since the development of HFD-mediated fibrosis/liver injury requires long treatments with an HFD (up to 7 months), it would be important to perform long-term studies with HFD treatments and test if cdk4 inhibitors might block the development of HFD-mediated fibrosis in this setting.

At this stage of investigation, it is important to note that we previously have examined ALT/AST in S193D and S193A mice (Jin et al., 2015; Wang et al., 2010), and we found that ALT and AST are elevated in S193D mice while they are reduced in S193A mice. It is likely that the less injury in S193A mice in the beginning of an HFD protocol might be involved in protection from NAFLD. It is interesting to mention that, while we have used relatively low doses of PD-0332991, we detected very strong prevention and reversion of steatosis within the time frame of 10 weeks of HFD treatments. It is also important to mention that, in reversal experiments, we kept feeding the HFD and PD-0332991 simultaneously for 5 weeks, and, despite HFD, the inhibitor of cdk4 dramatically reduced hepatic steatosis. This study gives great hope that cdk4-based therapy might be a worthy approach to treat patients with NAFLD, at least at early stages of the disease. Further studies with animals are required to test if cdk4 inhibitors might reverse late steps of NAFLD, such as fibrosis and NASH. Considering treatments of NAFLD patients with inhibitors of cdk4, it is important to keep in mind that, although PD-0332991 is a more specific inhibitor of cdk4, there is a risk for the development of liver cancer because it does not inhibit liver proliferation. From this point of view, inhibition of cdk4 by FPD might have a better outcome. In summary, our work elucidated the key event in the HFD-mediated NAFLD, and it provided the strong support for consideration of cdk4 inhibitors as a possible tool to treat NAFLD.

EXPERIMENTAL PROCEDURES

Animals

HFD Protocol

Experiments with animals were approved by the Institutional Animal Care and Use Committee (IACUC) at Baylor College of Medicine (protocol AN-1439) and by the IACUC at Cincinnati Children's Hospital (protocol IACUC2014-0042). In this study, we used 2- to 4-month-old WT, C/EBPα-S193D, and C/EBPα-S193A mice. Generation and characterization of C/EBPα-S193D and C/EBPα-S193A mice were described in our previous papers (Wang et al., 2010; Jin et al., 2010, 2013). Livers were harvested and kept at −80°C. For HFD experiments, mice and their age-matched littermate controls were fed either a standard laboratory chow diet or an HFD (D12331, Research Diets) for 3 or 12 weeks for a short-term study or for 20–48 weeks for long-term studies.

Inhibition of Cdk4 by FPD and PD-0332991

To inhibit activity of cdk4, we fed animals with inhibitors in chow diet (custom made by BioServ) ad libitum for 7 days prior to the initiation of an HFD protocol. After the 1-week pre-treatment, mice were given an HFD and were kept on the 0.025% FPD or PD-0332991 (in chow, 150 mg/kg chow) for 4 additional weeks. At the end of experiments, mice were sacrificed, and livers were examined for the development of hepatic steatosis and for the expression of genes as described below. Five mice per group of the protocol were used. In the reversal studies, we used four groups of mice (five mice/group, males). The protocol for reversal studies is summarized in Figure 7A.

Liver Histology and Immunohistochemistry

The livers were fixed overnight in buffered 10% formaldehyde, embedded in paraffin, and sectioned at a thickness of 5 μm. The sections were then stained with H&E using a standard protocol or with different antibodies against cdk4 (C-22, Santa Cruz Biotechnology). For oil red O staining of lipid droplets in frozen liver sections, the liver cryosections of 7 μm were stained with commercially available kits (IW-3008, IHC World). Sirius Red staining was performed using a Direct Red 80 (Sirius Red, Sigma-Aldrich) kit.

Antibodies and Reagents

Antibodies to C/EBPβ (C-19), C/EBPα (14AA), DGAT1 (H-255), DGAT2 (H-70), GPAT, PEPCK, G6-phase, p300 (N-15 or C-20), cdk4 (C-22), and cyclin D3 (C-16) were from Santa Cruz Biotechnology. Antibodies to FASN, SCD1, and ACC were from Cell Signaling Technology. Antibodies to Ser193-ph C/EBPα were purchased from Thermo Scientific (PA5-37342). Monoclonal anti-β-actin

antibody was from Sigma. CoIP studies were performed using TrueBlot reagents as previously described (Jin et al., 2013, 2015).

Protein Isolation and Western Blotting

Cytoplasmic and nuclear extracts were isolated from livers of mice as described previously (Wang et al., 2010; Jin et al., 2015). Inhibitors of phosphatases were included in all buffers used for the isolation of proteins or protein-protein complexes. Proteins (50–100 μg) were loaded on gradient (4%–20%) polyacrylamide gels, transferred onto membranes, and probed with antibodies against proteins of interest. To verify protein loading, each filter was re-probed with Abs to β-actin.

Real-Time qRT-PCR

Total RNA was isolated from mouse livers using RNEasy Plus mini kit (QIAGEN). The cDNA was synthesized with 2 μg total RNA using a High-Capacity cDNA Reverse Transcription Kit (Thermo Fisher Scientific). The cDNA was diluted five times with diethylpyrocarbonate (DEPC)-treated water and subsequently used for RT-PCR assays with the TaqMan Gene Expression system (Applied Biosystems). Gene expression analysis was performed using the TaqMan Universal PCR Master Mix (Applied Biosystems) in a total volume of 10 μl containing 5 μl Master Mix, 1.5 μl water, 3 μl cDNA template, and 0.5 μl of the gene-specific TaqMan Assay probe mixture. The cycling profile was 50°C for 2 min, 95°C for 10 min, followed by 40 cycles of 95°C for 15 s and 60°C for 1 min, as recommended by the manufacturer. TaqMan probe mixture for FXR (Mm00484523_m1), Gankyrin (Mm00450376_m1), and β-actin (Mm02619580-g1) was purchased from Applied Biosystems. All results were normalized to β-actin. Amplification and quantification were done with the Applied Biosystems StepOne Plus RT-PCR System.

Statistical Analysis

All values are presented as means ± SD. Statistical analyses were performed using the Student's t test. Statistical significance was assumed when $^{*}p < 0.05$ and $^{**}p < 0.01$.

SUPPLEMENTAL INFORMATION

Supplemental Information includes Supplemental Experimental Procedures and three figures and can be found with this article online at http://dx.doi.org/10.1016/j.celrep.2016.06.019.

AUTHOR CONTRIBUTIONS

J.J. and K.L. designed and performed experiments with examination of NAFLD in C/EBPα-S193A and C/EBPα-S193D mice. T.P.N., L.V., M.W., and A.C. designed and performed experiments with prevention and treatments of HFD-mediated hepatic steatosis by inhibitors of cdk4. L.S. and L.T. designed and performed ITT and examined expression of glucose and lipogenic enzymes. N.A.T. generated the ideas and supervised all studies. N.A.T., J.J., T.P.N., L.T., and L.V. wrote the paper.

ACKNOWLEDGMENTS

This work was supported by NIH grants R01DK102597 and R01CA159942 (N.A.T.), NIH grants AR052791 and AR064488 (L.T.), and Internal Development Funds from CCHMC (N.A.T. and L.T.). We thank Taeko Noah and Mary McKay for their assistance in experiments with mice and Holly Poling for help with immunostaining.

Received: December 28, 2015
Revised: March 18, 2016
Accepted: May 31, 2016
Published: June 30, 2016

REFERENCES

Anders, L., Ke, N., Hydbring, P., Choi, Y.J., Widlund, H.R., Chick, J.M., Zhai, H., Vidal, M., Gygi, S.P., Braun, P., and Sicinski, P. (2011). A systematic screen for CDK4/6 substrates links FOXM1 phosphorylation to senescence suppression in cancer cells. Cancer Cell *20*, 620–634.

Baker, S.J., and Reddy, E.P. (2012). CDK4: a key player in the cell cycle, development, and cancer. Genes Cancer *3*, 658–669.

Carr, R.M., and Reid, A.E. (2015). FXR agonists as therapeutic agents for non-alcoholic fatty liver disease. Curr. Atheroscler. *17*, 500.

Cohen, J.C., Horton, J.D., and Hobbs, H.H. (2011). Human fatty liver disease: old questions and new insights. Science *332*, 1519–1523.

Dickson, M.A., and Schwartz, G.K. (2009). Development of cell-cycle inhibitors for cancer therapy. Curr. Oncol. *16*, 36–43.

Endicott, J.A., Noble, M.E., and Tucker, J.A. (1999). Cyclin-dependent kinases: inhibition and substrate recognition. Curr. Opin. Struct. Biol. *9*, 738–744.

Flaherty, K.T., Lorusso, P.M., Demichele, A., Abramson, V.G., Courtney, R., Randolph, S.S., Shaik, M.N., Wilner, K.D., O'Dwyer, P.J., and Schwartz, G.K. (2012). Phase I, dose-escalation trial of the oral cyclin-dependent kinase 4/6 inhibitor PD 0332991, administered using a 21-day schedule in patients with advanced cancer. Clin. Cancer Res. *18*, 568–576, Published online Nov 16, 2011. http://dx.doi.org/10.1158/1078-0432.CCR-11-0509.

Fleet, T., Zhang, B., Lin, F., Zhu, B., Dasgupta, S., Stashi, E., Tackett, B., Thevananther, S., Rajapakshe, K.I., Gonzales, N., et al. (2015). SRC-2 orchestrates polygenic inputs for fine-tuning glucose homeostasis. Proc. Natl. Acad. Sci. USA *112*, E6068–E6077.

Gil, J., and Peters, G. (2006). Regulation of the INK4b-ARF-INK4a tumour suppressor locus: all for one or one for all. Nat. Rev. Mol. Cell Biol. *7*, 667–677.

Hebbard, L., and George, J. (2011). Animal models of nonalcoholic fatty liver disease. Nat. Rev. Gastroenterol. Hepatol. *8*, 35–44.

Hill-Baskin, A.E., Markiewski, M.M., Buchner, D.A., Shao, H., DeSantis, D., Hsiao, G., Subramaniam, S., Berger, N.A., Croniger, C., Lambris, J.D., and Nadeau, J.H. (2009). Diet-induced hepatocellular carcinoma in genetically predisposed mice. Hum. Mol. Genet. *18*, 2975–2988.

Jiang, Y., Iakova, P., Jin, J., Sullivan, E., Sharin, V., Hong, I.H., Anakk, S., Mayor, A., Darlington, G., Finegold, M., et al. (2013). Farnesoid X receptor inhibits gankyrin in mouse livers and prevents development of liver cancer. Hepatology *57*, 1098–1106.

Jin, J., Wang, G.L., Iakova, P., Shi, X., Haefliger, S., Finegold, M., and Timchenko, N.A. (2010). Epigenetic changes play critical role in age-associated dysfunctions of the liver. Aging Cell *9*, 895–910.

Jin, J., Iakova, P., Breaux, M., Sullivan, E., Jawanmardi, N., Chen, D., Jiang, Y., Medrano, E.M., and Timchenko, N.A. (2013). Increased expression of enzymes of triglyceride synthesis is essential for the development of hepatic steatosis. Cell Rep. *3*, 831–843.

Jin, J., Hong, I.H., Lewis, K., Iakova, P., Breaux, M., Jiang, Y., Sullivan, E., Jawanmardi, N., Timchenko, L., and Timchenko, N.A. (2015). Cooperation of C/EBP family proteins and chromatin remodeling proteins is essential for termination of liver regeneration. Hepatology *61*, 315–325.

Johnson, P.F. (2005). Molecular stop signs: regulation of cell-cycle arrest by C/EBP transcription factors. J. Cell Sci. *118*, 2545–2555.

Leonard, J.P., LaCasce, A.S., Smith, M.R., Noy, A., Chirieac, L.R., Rodig, S.J., Yu, J.Q., Vallabhajosula, S., Schoder, H., English, P., et al. (2012). Selective CDK4/6 inhibition with tumor responses by PD0332991 in patients with mantle cell lymphoma. Blood *119*, 4597–4607, Published online Mar 1, 2012. http://dx.doi.org/10.1182/blood-2011-10-388298.

Luke, J.J., D'Adamo, D.R., Dickson, M.A., Keohan, M.L., Carvajal, R.D., Maki, R.G., de Stanchina, E., Musi, E., Singer, S., and Schwartz, G.K. (2012). The cyclin-dependent kinase inhibitor flavopiridol potentiates doxorubicin efficacy in advanced sarcomas: preclinical investigations and results of a phase I dose-escalation clinical trial. Clin. Cancer Res. *18*, 2638–2647.

Nagaria, T.S., Williams, J.L., Leduc, C., Squire, J.A., Greer, P.A., and Sangrar, W. (2013). Flavopiridol synergizes with sorafenib to induce cytotoxicity and potentiate antitumorigenic activity in EGFR/HER-2 and mutant RAS/RAF breast cancer model systems. Neoplasia *15*, 939–951.

Rivadeneira, D.B., Mayhew, C.N., Thangavel, C., Sotillo, E., Reed, C.A., Graña, X., and Knudsen, E.S. (2010). Proliferative suppression by CDK4/6 inhibition: complex function of the retinoblastoma pathway in liver tissue and hepatoma cells. Gastroenterology *138*, 1920–1930.

Schmucker, D.L. (2005). Age-related changes in liver structure and function: Implications for disease? Exp. Gerontol. *40*, 650–659.

Timchenko, N.A. (2009). Aging and liver regeneration. Trends Endocrinol. Metab. *20*, 171–176.

Timchenko, N.A. (2011). Senescent liver. In Molecular Pathology of Liver Diseases, S.P.S. Monga, ed. (Springer Science + Business Media), pp. 279–290.

Vansaun, M.N., Mendonsa, A.M., and Lee Gorden, D. (2013). Hepatocellular proliferation correlates with inflammatory cell and cytokine changes in a murine model of nonalchoholic fatty liver disease. PLoS ONE *8*, e73054.

Wang, G.-L., and Timchenko, N.A. (2005). Dephosphorylated C/EBPalpha accelerates cell proliferation through sequestering retinoblastoma protein. Mol. Cell. Biol. *25*, 1325–1338.

Wang, G.-L., Shi, X., Salisbury, E., Sun, Y., Albrecht, J.H., Smith, R.G., and Timchenko, N.A. (2006). Cyclin D3 maintains growth-inhibitory activity of C/EBPalpha by stabilizing C/EBPalpha-cdk2 and C/EBPalpha-Brm complexes. Mol. Cell. Biol. *26*, 2570–2582.

Wang, G.-L., Shi, X., Haefliger, S., Jin, J., Major, A., Iakova, P., Finegold, M., and Timchenko, N.A. (2010). Elimination of C/EBPalpha through the ubiquitin-proteasome system promotes the development of liver cancer in mice. J. Clin. Invest. *120*, 2549–2562.

Xu, J.Y., Li, Z.P., Zhang, L., and Ji, G. (2014). Recent insights into farnesoid X receptor in non-alcoholic fatty liver disease. World J. Gastroenterol. *20*, 13493–13500.